Molecular Phylogenetics and Evolution 70 (2014) 492–503

Contents lists available at ScienceDirect

Molecular Phylogenetics and Evolution

journal homepage: www.elsevier.com/locate/ympev

The origin of the early differentiation of Ivies (*Hedera* L.) and the radiation of the Asian Palmate group (Araliaceae)

Virginia Valcárcel [a,*], Omar Fiz-Palacios [b], Jun Wen [c]

[a] Universidad Autónoma de Madrid, Campus Canto Blanco, C./ Darwin 2, 28049 Madrid, Spain
[b] Evolutionary Biology Centre, Norbyvägen 18 D, Uppsala 75236, Sweden
[c] Department of Botany/MRC 166, Smithsonian Institution, PO Box 37012, Washington, DC 20013-7012, USA

ARTICLE INFO

Article history:
Received 8 August 2013
Revised 18 October 2013
Accepted 22 October 2013
Available online 30 October 2013

Keywords:
Araliaceae
Early radiation
Hedera
Temperate
Tropical
Upper Cretaceous cooling

ABSTRACT

The Asian Palmate group is one of the four major clades of the family Araliaceae that is formed by 18 genera, including ivies (*Hedera* L.). The Mediterranean diversity centre and temperate affinity of ivies contrast with the inferred Asian centre of diversity of the primarily tropical and subtropical Asian Palmate group. We herein investigated the sister-group relationships of *Hedera* to reconstruct the evolutionary context for its origin and early diversification. Seven nuclear and plastid DNA regions were analyzed in 61 Araliaceae samples including all the 18 Asian Palmate genera. Maximum Parsimony, Maximum Likelihood and Bayesian Inference were run together with a battery of topology testing analyses constraining the expected *Hedera's* sister-group relationships. Additionally, Bayesian polytomy resolvability and divergence time analyses were also conducted. Genome incongruence and hard nuclear and plastid basal polytomies are detected for the Asian Palmate group where the lineage of *Hedera* is placed. Topology testing analyses do not allow rejecting any of the tentative sisters of *Hedera*. An early radiation with inter-lineage hybridization and genome doubling is suggested for the Asian Palmate group where all the seven temperate genera, including *Hedera*, seem to have played an important role. The radiation took placed during the Upper Cretaceous in Asia under a general cooling and the eastern Asian mountain uplift that produced new temperate environments and promoted lineage connections. This allows us to hypothesize that the origin of the *Hedera* lineage may fit in a temperate niche conservatism scenario where the combination of the radiation with lineage admixtures prevents us from discovering its sister-group.

1. Introduction

The family Araliaceae in its modern circumscription constitutes a monophyletic lineage largely congruent with the conventional delimitation of the family (Mitchell et al., 2012; Plunkett et al., 2004). Only two tribes traditionally considered within Araliaceae (*Mackinlayeae,* Harms, 1898; Mackinlayaceae, Doweld, 2001; and *Myodocarpeae*, Calestani, 1905; Viguier, 1906; Myodocarpaceae, Doweld, 2001) appear out of the core as two independent lineages (Chandler and Plunkett, 2004; Plunkett and Lowry, 2001; Plunkett et al., 2004). As a result, 41 genera are now considered in the Araliaceae (Mitchell et al., 2012; Plunkett et al., 2004). Phylogenetic reconstructions of the Araliaceae reveal three main clades (Asian Palmate, *Aralia–Panax* and *Polyscias–Pseudopanax*) placed in a basal polytomy together with a group of poorly resolved minor lineages (Plunkett et al., 2004; Wen et al., 2001). A recent study has revealed a new fourth main clade also placed in the basal polytomy (Greater *Raukaua* clade, Mitchell et al., 2012). None of these four main clades has any congruence with the tribes traditionally recognized based on morphology (Plunkett et al., 2004; Wen et al., 2001). However, a geographical pattern is detected with two of the four main clades centered in Southeast Asia (Asian Palmate and *Aralia–Panax* groups) and the remaining two in the Pacific and Indian Ocean basin (Greater *Raukaua* and *Polyscias–Pseudopanax* group, Mitchell et al., 2012; Plunkett et al., 2004; Wen et al., 2001). The basal polytomy and short internal branches retrieved in the phylogenies of the Araliaceae have been interpreted as a result of a period of fast proliferation of lineages linked to the break-up of Gondwana (Plunkett et al., 2004; Yi et al., 2004). The first divergence time estimates of the family partially confirmed this hypothesis since the Araliaceae crown age coincides with the end of the break-up of Gondwana (*c.* 84 mya; Mitchell et al., 2012).

Eighteen morphologically diverse genera have been traditionally included in the Asian Palmate group (Plunkett et al., 2004; Wen et al., 2001; Fig. 1). However, the total number of genus-level

* Corresponding author. Fax: +34 914978344.
E-mail addresses: virginia.valcarcel@uam.es (V. Valcárcel), fizpal@googlemail.com (O. Fiz-Palacios), WENJ@si.edu (J. Wen).

1055-7903/$ - see front matter © 2013 Elsevier Inc. All rights reserved.
http://dx.doi.org/10.1016/j.ympev.2013.10.016

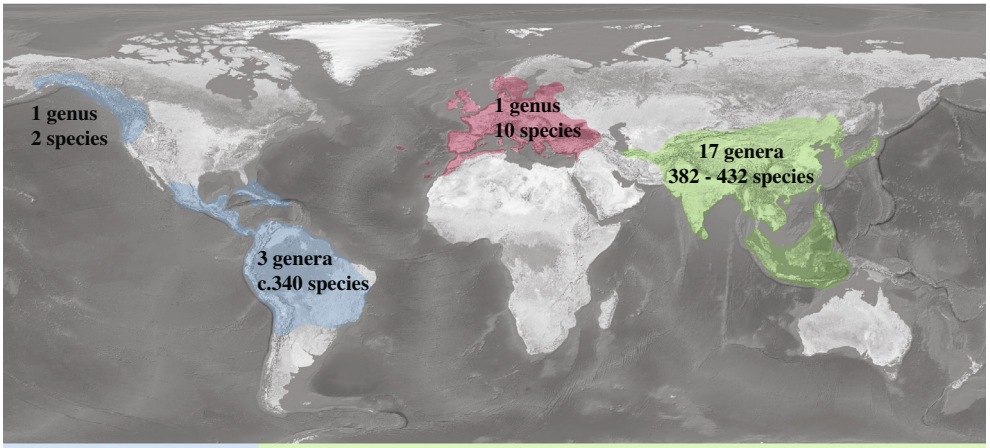

*Dendropanax** (c.60)	Asian *Schefflera* (250 - 300)	*Fatsia* (3)	*Macropanax* (14)	**Tetrapanax (1)**
Oplopanax* (2)	*Brassaiopsis* (25)	**Gamblea (4)**	*Merrilliopanax* (4)	*Trevesia* (c.10)
Oreopanax (80)	**Chengiopanax (2)**	**Hedera* (2)**	*Metapanax* (2)	
Neotropical *Schefflera* (c.200)	*Dendropanax** (c.25)	*Heteropanax* (7)	**Oplopanax* (1)**	
Hedera* (10)	**Eleutherococcus (30)**	**Kalopanax (1)**	*Sinopanax* (1)	

Fig. 1. Worldwide distribution of the Asian Palmate genera. The genera are arranged by geographical areas indicating the number of species per genus and geographical area in parenthesis. Temperate genera are highlighted in bold. Asterisks indicate genera with inter-continental disjunction.

lineages is 20. This is due to the split of the: (1) Old World species of *Dendropanax* (*Dendropanax* subgen. *Textoria*, Li and Wen, 2013) into two separate clades (the *Dendropanax hainanensis* clade *vs.* the remaining *Dendropanax* subgen. *Textoria*; Li and Wen, 2013) and (2) Scheffleras included in the Asian Palmante group into the Neotropical and the Asian *Schefflera* subgroups (Fiaschi and Plunkett, 2011; Plunkett et al., 2004, 2005). Aside from the palmate-like leaves, there is only one morphological character (unarticulated pedicels) that is shared by all the 18 genera of the group except for *Macropanax* and *Metapanax* (Plunkett et al., 2004). In addition to this scant morphological affinity and the above-described geographical congruence it is interesting to notice that most of the members of the Asian Palmate group are polyploids (Yi et al., 2004). In fact, 14 of the 18 Asian Palmate genera with chromosome counted to date are tetraploids, three of which also have diploid species placed in terminal positions (Yi et al., 2004). Interestingly, members of the remaining three main clades of the family are diploids (*Aralia–Panax*, greater *Raukaua* and *Polyscias–Pseudopanax* groups). Considering all this, Yi et al. (2004) proposed either (1) a single polyploidization event at the origin of the Asian Palmate group followed by at least three independent reversals to the diploid condition or (2) a diploid origin followed by multiple independent polyploidyzations affecting all main lineages within the group. However, the basal polytomy also retrieved for the Asian Palmate group prevented the authors from setting up the most likely scenario.

The genus *Hedera* has 12 extant species (Valcárcel and Vargas, 2010) with a range that extends from Macaronesia to Japan throughout North Africa, Europe, and continental Asia. Its phylogenetic placement is indisputably within the Asian Palmate group, although the closest relatives remain unknown (Lowry et al., 2001; Plunkett and Lowry, 2001; Plunkett et al., 2004; Valcárcel et al., 2003; Valcárcel, 2008; Wen et al., 2001; Yi et al., 2004). Disclosing the sister-group of *Hedera* is challenging since ivies barely share any geographical, ecological or morphological affinity with the remaining members of the Asian Palmate group. Indeed, 13 of the 18 Asian Palmate genera are restricted to Asia while the distribution of *Hedera* extends to Europe (Fig. 1). The remaining four Asian Palmate genera with an extra-Asian range occur in the New World (*Dendropanax, Oplopanax, Oreopanax*, *Schefflera;* Fig. 1). Besides, *Hedera,* together with six other genera of the group (*Chengiopanax*, *Eleutherococcus*, *Gamblea*, *Kalopanax*, *Oplopanax*, and *Tetrapanax;* Fig. 1) display a north temperate distribution. This latitudinal range contrasts with the strict tropical/subtropical affinity of the remaining 11 genera. Finally, while the diversity centre of the whole Asian Palmate group and some of its genera (*Dendropanax* subgen. *Textoria, Trevesia, Brassaiopsis*) have been located in tropical/subtropical Southeast Asia (Fig. 1; Li and Wen, 2013; Mitchell and Wen, 2005; Mitchell et al., 2012; Plunkett et al., 2004; Wen et al., 2001, 2007), the primary center suggested for ivies has been placed in the Mediterranean basin (Ackerfield and Wen, 2003; Green et al., 2011; Valcárcel et al., 2003; Valcárcel and Vargas, 2013; Vargas et al., 1999). Unfortunately, phylogenetic studies have systematically failed to infer *Hedera* sister-group, and thus to reconstruct its origin and early divergence. Four different lineages of the Asian Palmate group are consistently suggested as putative sister-groups although with marginal support: (i) *Trevesia-Brassaiopsis* group (Lowry et al., 2001; Plunkett and Lowry, 2001; Plunkett et al., 2004; Valcárcel et al., 2003; Wen et al., 2001; Yi et al., 2004), (ii) *Dendropanax* (Li and Wen, 2013; Valcárcel, 2008), (iii) *Kalopanax* (Chandler and Plunkett, 2004), and (iv) *Merrillionapax* (Mitchell and Wen, 2004; Mitchell et al., 2012; Plunkett et al., 2004). The sister-group relationship between *Hedera* and the *Trevesia-Brassaiopsis* group is supported by morphology. Traditional taxonomy of the family Araliaceae has related *Hedera* within a reduced group of genera with single styles that includes *Brassaiopsis* (Seemann, 1868). Additionally, both genera share smooth fruits (Frodin and Govaerts, 2003), similar multicellular foliar trichomes (Ackerfield, 2001; Lum and Maze, 1989; McAllister and Rutherford, 1990; Valcárcel and Vargas, 2010; Wen et al., 2003) and lobed leaves (Mitchell and Wen, 2005; Valcárcel and Vargas, 2010). Morphology does also support the association between *Hedera* and *Dendropanax* since they both have single styles (Seemann, 1868), 3–5 carpels (Li and Wen, 2013; Valcárcel, 2008) and entire to (2)3–5(7) lobed leaves (Li and Wen, 2013; Valcárcel, 2008). Limited morphological affinity does

also support the putative sister-group relationship between *Hedera* and *Merrilliopanax* due to their simple and lobed leaves, while major differences regarding carpels, style and the organization of the inflorescence do also exists. The remaining alternative sister-group suggested for *Hedera* (*Kalopanax*) is instead supported by niche similarity since this genus also displays a north temperate distribution. However, the poor internal resolution of the Asian Palmate group phylogeny (Mitchell et al., 2012; Plunkett et al., 2004; Valcárcel et al., 2003; Wen et al., 2001) has systematically precluded revealing the closest relatives of *Hedera*.

In the present study we investigated the sister-group relationships of *Hedera* to reconstruct the evolutionary context for its origin and early diversification. For this purpose we analyzed a multi-gene dataset including one nuclear (ITS) and six plastid regions (*atpB-rbcL*, *ndhF*, *psbA-trnH*, *rps*16, *rpl*16, *trnL-trnF*) from 49 representatives of all the 18 Asian Palmate genera plus 12 species of non-Asian Palmate genera of Araliaceae. We evaluated the sister-group relationships of *Hedera* inferring phylogenetic reconstructions for the Asian Palmate group under Maximum Parsimony, Maximum Likelihood and Bayesian methods. Based on the already suggested putative sisters we propose two competing hypotheses for the early divergence of the *Hedera* lineage: "tropical conservatism" under which the sister of *Hedera* would be a tropical or subtropical genus and the divergence of *Hedera* would be related to the acquisition of new temperate requirements; "phylogenetic niche conservatism" under which the lineage of *Hedera* would have retained ecological traits with its temperate sister over time. Additionally, we considered a third hypothesis ("radiation hypothesis") in which the ancestor of *Hedera* was involved in a radiation with new lineages successful in different ecological and distribution areas. Our expectations for *Hedera* sisters under the three alternative hypotheses are: (1) *Dendropanax,* the *Trevesia-Brassaiopsis* group, or *Merrilliopanax* for the tropical conservatism hypothesis; (2) *Kalopanax* for phylogenetic niche conservatism; or (3) no sister recovered under the radiation hypothesis. To incorporate the radiation scenario into the phylogenetic searches we also conducted analyses of resolvability for the internal nodes of the phylogeny using a reversible-jump MCMC approach that allows polytomous trees as true trees during the search. Finally, we estimated divergence times for main nodes of the Asian Palmate clade to integrate the alternative sister-group topologies into a temporal framework and evaluate the competing hypotheses.

2. Materials and methods

2.1. Sampling and alignment

Sixty-one samples were included in the present study: 49 of the Asian Palmate group and 12 of the remaining main clades of Araliaceae (*Aralia–Panax*, and *Polyscias–Pseudopanax*, Supplementary Table 1). *Harmsiopanax ingens* was used as the outgroup in all the phylogenetic analyses. The 49 samples of the Asian Palmate group included represent all the 18 genera (1–5 species per genus) including the two independent lineages of: (1) *Dendropanax* subgen. *Textoria* and (2) Asian Palmate lineages of *Schefflera*.

Seven DNA markers were analyzed: the internal transcribed spacer (ITS) from the nrDNA, three non-coding plastid DNA markers (*atp*B-*rbc*L, *psb*A-*trn*H, and *trn*L-*trn*F), and three coding plastid DNA markers (NADH dehydrogenase subunit F, ribosomal protein L16, and ribosomal protein S16). The sequences of the seven DNA regions of 52 species were taken from previous works (Mitchell and Wen, 2005; Mitchell et al., 2012; Li and Wen, 2013) and downloaded from the GenBank database (http://www.ncbi.nlm.nih.gov). Sixty-six new sequences were obtained in the present study for 11 species to complete taxonomic sampling gaps (Supplementary Table 1). Amplifications and sequencing protocols were done according to Mitchell et al. (2012).

Seven independent DNA matrices corresponding to the seven DNA markers were compiled with the same 61 samples (Supplementary Table 1). Matrix alignments were carried out with MUSCLE (Edgar, 2004) followed by manual revision in Geneious v4.7 (http://www.genious.com). The six-plastid matrices were concatenated with the program Sequence Matrix (Vaidya et al., 2010) into one single matrix (hereafter called "plastid matrix").

2.2. Unconstrained phylogenetic analyses

A set of three unconstrained analyses were run from the ITS and the plastid matrices independently (Maximum Parsimony, MP; Bayesian Inference, BI; and Maximum Likelihood, ML). Maximum Parsimony analyses were run under no constraints as implemented in the program TNT (Goloboff et al., 2003) using heuristic traditional searches with random starting trees and tree bisection-reconnection branch swapping. An initial search with 9×10^5 random addition replicates was run retaining ten trees per replicate. Once the initial search finished, swapping was completed on the trees retained in the previous analysis. The nonparametric bootstraps were calculated with traditional searches using 10^3 bootstrap replicates and 10^5 random additions per replicate. For the remaining phylogenetic analyses selection of the evolutionary model that best fits the nine regions of the seven DNA markers (ITS1, 5.8S, ITS2, *atp*B-*rbc*L, *psb*A-*trn*H, *trn*L-*trn*F, NADH dehydrogenase subunit F, ribosomal protein L16, and ribosomal protein S16) was performed as implemented in the program jModeltest 1.1b (Posada, 2008). Three substitution type models were evaluated with the second order AIC (AICc, Hurvich and Tsai, 1989). Model selection uncertainty was evaluated by analyzing AICc values and weights (Posada and Buckley, 2004). Partitions of the ITS and plastid matrices were applied according to the best fitting evolutionary models selected (Supplementary Table 2) as well as to the individual gene trees concordance (Rannala and Yang, 2008). The BI analyses were performed as implemented in MrBayes 3.2.1 (Huelsenbeck and Ronquist, 2001). Computations of the BI analyses were run on the computer cluster of the Cyber-Infrastructure for Phylogenetic Research project (CIPRES, www.phylo.org) at the San Diego Supercomputer Center. Two runs with four Markov chain Monte Carlo (MCMC) iterations were performed over 50×10^6 generations. Trees were sampled every 10^3 generations and branch lengths were retained. Likelihood convergence was determined with TRACER v1.4 (Rambaut and Drummond, 2007). Topological convergence was checked with AWTY (Wilgenbusch et al., 2004). Trees retrieved before reaching the likelihood and topological convergence were discarded. The ML analyses were performed using CATGAMMA model with 10^4 bootstrap replicates as implemented in RAxML-VI-HPC (Stamatakis et al., 2008; software available at www.epfl.ch/~stamatak). Two additional BI analyses were run by removing terminals with long branches from the ITS and plastid matrices.

Incongruence tests were performed to check for the adequacy of concatenating the nuclear and the plastid sequences to conduct further MP, ML and BI analyses. The incongruence length different test (ILD; Mickevich and Farris, 1981) and Approximate Unbiased test (AU; Shimodaira, 2002) were used to explore discordance. The ILD test was performed as the script implemented in TNT by using 10^3 replicates and Tree Bisection Reconnection algorithm. The ILD test is one of the most widely used methods for assessing incongruence, however it suffers from high false positives (Hipp et al., 2004). The AU test is very conservative when rejecting the null hypothesis (i.e., all the trees under evaluation are equally good) and has been proven to perform better than other nonparametric bootstraping methods (Planet, 2006). The AU test was

performed as implemented in Treefinder (Jobb et al., 2004; Jobb, 2007). The likelihood of the majority-rule consensus tree obtained from the unconstrained BI of the ITS and the plastid matrices were compared using 10^5 replicates and partitioning datasets. The competing hypotheses were rejected at a significance level of 0.05.

Concatenating sequences from multiple loci results in wrong estimation of the species tree in cases of gene trees incongruence (Degnan and Rosenberg, 2006). This is particularly true when the incongruence is attributable to incomplete lineage sorting (Heled and Drummond, 2010). A species tree was estimated from the nine DNA partitions (ITS1, 5.8S, ITS2, atpB-*rbc*L, *ndh*F, *psb*A-*trn*H, *rpl*16, *rps*16, *trn*L-*trn*F) using *BEAST (Heled and Drummond, 2010) as implemented in BEAST v. 1.7.4 (Drummond and Rambaut, 2007). *BEAST employs a Bayesian method that assesses multispecies coalescence by estimating the coalescent in the extant and ancestral species from each of the multiple gene trees contained within the same species tree. The DNA partitions were unlinked for the substitution, tree and clock model estimates and Yule model was set for the species tree prior. MCMC was run for 5×10^7 generations sampling every 10^3 generations. Likelihood and topological convergence were assessed with TRACER v1.4 (Rambaut and Drummond, 2007) and AWTY (Wilgenbusch et al., 2004). Trees retrieved before reaching convergence were discarded.

We ran additional Bayesian analyses as implemented in Phycas 1.2.0 (Lewis et al., 2010) to estimate the posterior probability of internal nodes being polytomies (Nagy et al., 2012). Phycas uses a reversible-jump MCMC algorithm that allows jumping between trees with different levels of resolution. Therefore it allows the inclusion of polytomous trees in the searching process. Two polytomy class priors were applied: (1) the polytomy class and (2) the resolution class. The polytomy class prior accounts for the relative prior probability of a tree with *m* internal nodes and an *m-1* internal nodes tree. The resolution class prior considers both the number of internal nodes per tree and the number of possible trees with a particular number of internal nodes. Therefore, the resolution class corrects the biased towards a larger number of completely resolved trees than polytomous ones for any given *i*-terminals. We explored the effects of three tree topology priors (C = 1, C = 2, C = 10; Lewis et al., 2005) both using the polytomy class prior and the resolution class prior. Setting the topology prior C to 1 results in a flat prior while setting C values >1 favors trees with less resolved topologies. As a result we ran 12 Bayesian analyses, six with the ITS matrix and six with the plastid one. Each MCMC was run for 10^5 cycles sampling trees every 10th cycle (1 cycle equals ca. 200 traditional Bayesian generations; Lewis et al., 2010). The 30% initial trees were discarded after checking for convergence with TRACER and AYWT. Due to lack of topological convergence the final analyses for the plastid matrix were run for 3×10^5 cycles.

2.3. Hypotheses testing of the sister-groups of Hedera

A set of hypothesis testing analyses was run to evaluate the most probable sister-group of *Hedera*. Five alternative phylogenetic hypotheses representing five possible sister-groups of *Hedera* were built: four based on previous studies (*Dendropanax* subgen. *Textoria pro parte, Trevesia-Brassaiopsis* group, *Kalopanax*, and *Merrillionapax*) plus a new one recovered in the present study (Table 1). The five alternative phylogenetic trees were inferred in MrBayes both from the ITS and the plastid matrices independently by applying topological constraints. We compared the ITS and plastid majority rule consensus tree obtained in the unconstrained BI analyses against the alternative phylogenetic hypotheses. As a result, we run 10 constrained BI analyses following the procedure specified above with 10^7 generations. Comparison of unconstrained and constrained topologies was performed both using the Bayes Factors (BF; Kass and Raferty, 1995; Suchard et al., 2001) and the AU test (Shimodaira, 2002). The BF analysis allows comparing the strength of evidence between a reference model (H_0) and an alternative model (H_i) given the data. To estimate the marginal likelihoods of the hypotheses under evaluation we used the stepping-stone sampling method (Xie et al., 2011) as implemented in MrBayes 3.2 (Ronquist et al., 2012). The stepping-stone method provides more accurate estimates than the harmonic mean method (Xie et al., 2011; Bergsten et al., 2013). The sampling was performed for 50 steps with 200,000 generations per step in two independent parallel MCMC runs, setting burn-into 60 samples. Convergence was examined through diagnostic plots of standard deviation of the split frequencies and screening similarity in the two independent marginal likelihood estimates (Ronquist et al., 2011). Selection of the best competing hypotheses against the H_0 (i.e., the unconstrained BI phylogenies) was based on the natural log Bayes Factors (LBF = $2\log_e$(BF)) evidence interpreted according to the table of Kass and Raftery (1995; Positive evidence, $2\log_e$(BF) = 2–6; Strong evidence, $2\log_e$(BF) = 6–10; Very Strong evidence, $2\log_e$(BF) > 10). Positive values of the LBF indicate preference for H_1, while negative values favor the H_0. The likelihood of the majority-rule consensus tree obtained from the unconstrained and constrained BI analyses were computed for the AU test following the procedure above described.

2.4. Divergence age analyses

Two calibration points were applied based on the fossils used by Li and Wen (2013) following a uniform distribution: (1) the stem lineage of *Metapanax* was calibrated to be 44–44.2 mya old based on the fruit fossil of *Paleopanax oregonensis* (Manchester, 1994), and (2) the crown age for the *Aralia elata* group (*A. elata, A. finlaysoniana, A. vietnamensis*) was calibrated to be 11.2–11.4 mya old based on fossil seeds similar to those of the extant *Aralia elata* (Szafer, 1961). A third calibration was applied for the ITS analyses setting the crown of the ingroup (Asian Palmate group) to a maximum age of 62 myr according to previous results (Mitchell et al., 2012) and our plastid age estimates.

Estimation of divergence times was carried out in two steps. The first step consisted of two topologically unconstrained age estimations, one for the ITS matrix and one for the plastid. Divergence times for these unconstrained analyses were estimated under the uncorrelated lognormal model in BEAST v.1.7.4

Table 1
Competing hypotheses under evaluation. Each hypothesis represents the scenario for the early divergence of the *Hedera* lineage based on the expected sister-groups of *Hedera*.

Hypothesis	*Hedera* sister to	Reference
Radiation	*No sister recovered*	Present study
Phylogenetic niche conservatism	*Kalopanax*	Chandler and Plunkett (2004), Present study
Tropical conservatism	*Dendropanax*	Mitchell and Wen (2005)
	Merrilliopanax	Mitchell and Wen (2004), Plunkett et al. (2004), Present study
	Trevesia-Brassaiopsis group	Plunkett et al. (2004), Valcárcel et al. (2003)
Phylogenetic niche conservatism/Tropical conservatism	*Eleutherococcus, Neotropical Schefflera*	Present study

(Drummond and Rambaut, 2007). Thirty million generations were simulated sampling every 10^3 generation. The GTR model was applied for the plastid and ITS analyses. Convergence of the MCMC-chains was estimated with TRACER v1.4 (Rambaut and Drummond, 2007). Final chronograms were produced with TreeAnnotator v1.5.4 after discarding generations before convergence.

The second step consisted of a set of divergence age estimations using topologically constrained input trees. This second step was performed to evaluate the stem age of *Hedera*. The topology of the ITS and plastid chronograms obtained in the unconstrained BEAST analyses was modified in Mesquite (Maddison and Maddison, 2011). Four of the five *Hedera* sister-groups were evaluated. Selection of the four *Hedera* sisters used was done based on the results of the BF and AU test to represent: (1) the topologies retrieved in the unconstrained ITS and plastid analyses, and (2) the two resolved topologies under evaluation (tropical conservatism and phylogenetic niche conservatism). Molecular clock analysis were then performed using MCMCTREE (Rannala and Yang, 2007; Yang and Rannala, 2006) as inplemented in PALM v.4.4 (Yang, 2007). The root of the tree was forced to be <121 mya, while the two calibrations above mentioned were constrained to soft bound of 11.2–11.4 mya and 44–44.2 mya. Divergence times were estimated under the independent rates model, with the gamma prior on the overall substitution rate specified as G (1,2) for plastid and G(1,11) for ITS, where the shape parameter was fixed ($a = 1$) to represent a diffuse prior and where the mean rate was estimated using CODEML (Yang, 2007). Fifteen million iterations sampling every 75 were run and 1,5 millions were discarded as burn-in.

3. Results

3.1. Phylogenetic reconstructions: gene trees and species tree

The BI, MP and ML phylogenetic analyses of the nuclear ITS region reveal differences in clade supports that affected tree topologies (Fig. 2; Supplementary Figs. 1 and 2). The Asian Palmate group is a well-supported monophyletic clade with a large basal polytomy (92% bootstrap (BS) in MP, 98% BS in ML and 1.0 posterior probabilities (PP) in BI; Fig. 2). *Hedera* is monophyletic (100% BS in MP and ML, 1.00 PP in BI; Fig. 2). No sister-group is recovered for *Hedera* since it is placed in the basal polytomy of the Asian Palmate group (Fig. 2). However, the BI and ML analyses suggest a relationship between *Hedera* and *Kalopanax* although with low support (<0.75 PP in BI; <50% BS in ML; Fig. 2; Supplementary Fig. 2).

The BI, MP and ML phylogenetic analyses of the plastid matrix reveal differences in clade supports that affected tree topologies (Fig. 3; Supplementary Figs. 3 and 4). Monophyly of the Asian Palmate group is supported both by the ML (82% BS) and BI (1.00 PP) analyses (Fig. 3). *Oplopanax elatus* is sister to a large clade that includes the remaining 17 genera of the Asian Palmate group. This main clade is divided in two subclades: one including *Heteropanax*, *Tetrapanax* and the Asian *Schefflera* and the other one including all the remaining genera (hereafter "*Eleutherococcus* clade", Fig. 3). The *Eleutherococcus* clade presents a large basal polytomy (Fig. 3). The monophyly of *Hedera* is highly supported (1.00 PP, 100% BS in ML and MP; Fig. 3). No sister is recovered for *Hedera* since it is placed in the large basal polytomy of the *Eleutherococcus* clade (Fig. 3). The MP analysis suggests a relationship between *Hedera* and *Merrilliopanax* although the support was low (<50% BS in ML; Supplementary Fig. 3). On the other hand, the BI and ML analyses suggest two possible sisters but with no support: *Eleutherococcus* or the Neotropical *Schefflera* (*Schefflera angulata, S. pentandra and S. morototoni*; Fig. 3, and Supplementary Fig. 4).

The ILD reveals significant incongruence between the ITS and plastid matrices. The plastid topology was rejected by the ITS dataset as revealed by the AU test results (difference in – LnL = 104.443, $p < 0.001$). Similarly, the ITS topology was rejected by the plastid dataset as revealed by the AU test results (difference in – LnL = 246.32, $p < 0.001$). Indeed, few major incongruence are observed between the ITS and plastid phylogenetic reconstructions. The first major incongruence affects the temperate *Oplopanax elatus* which appears at the base of the plastid tree and sister to the remaining 17 Asian Palmate genera while sister to *Fatsia* in a terminal position of the ITS phylogeny (compare node 3 in Figs. 3 and 2). The placement of *Oplopanax* in the species tree obtained with *BEAST is consistent with the one revealed by the plastid topology (Supplementary Fig. 5). The second major incongruence affects the placement of the temperate genera *Gamblea innovans* and *Chengiopanax fargesii* that are sisters in the ITS phylogeny (see node 1 in Fig. 2) but completely separated in independent lineages in the plastid one (see nodes 1a and 1b in Fig. 3). Phylogenetic placement of both genera is unresolved and placed in the basal polytomy of the *Eleutherococcus* clade according to species tree obtained with *BEAST (Supplementary Fig. 5). The third major incongruence affects the tropical/subtropical *Macropanax–Metapanax* clade that appears as sister to the temperate genera *Eleutherococcus* in the ITS phylogeny and *Kalopanax* in the plastid phylogeny (compare node 2 in Figs. 2 and 3). The placement of the *Macropanax–Metapanax* clade in the species tree obtained with *BEAST is congruent with the one revealed by the plastid topology (Supplementary Fig. 5).

The ITS and plastid phylogenetic analyses conducted after removing *Tetrapanax* and *Oplopanax* because of their long branches, reveal identical reconstructions and same level of genomes incongruence (difference in – LnL = 193.62, $p < 0.001$).

3.2. Analyses of synapomorphies

The ITS polytomy analysis reveals major incongruence between genera. The number of informative sites between genera within the Asian Palmate group is 101 (31 synapomorphies) while it is 44 within genus (28 synapomorphies) (Supplementary Table 3). The analysis of the 31 between-genera synapomorphies reveals incongruence. The genus *Hedera* is supported by 11 synapomorphies. Seven between-genera synapomorphies are detected for *Hedera*, each of which supports a different genus-lineage affinity.

The plastid polytomy analysis also reveals incongruence. Within the Asian Palmate group the number of potentially informative characters are 89 (33 synapomorphies) between genera and 103 (61 synapomorphies) within genus (Supplementary Table 3). The number of informative characters between genera of the *Eleutherococcus* clade is 80 (24 synapomorphies), while 98 within-genus (57 synapomorphies). Sixteen of the 24 between-genera synapomorphies detected within the *Eleutherococcus* clade reveal incongruent patterns. Incongruent sites primarily affect eight genera (*Dendropanax* subgen. *Textoria pro parte, Eleutherococcus,* Neotropical *Schefflera, Hedera, Fatsia, Sinopanax, Oreopanax,* and *Merrilliopanax*). The genus *Hedera* is supported by nine synapomorphies. The two between-genera synapomorphies detected for *Hedera* reveal incongruences.

3.3. Polytomy resolvability analyses

The ITS resolvability analyses provided high support (PP $\geqslant$ 0.95) for incongruent nodes 2 and 3 (Fig. 2) irrespective of the topology prior used, except for node 2 that is dissolved when using the highest topology prior (Supplementary Table 4). The node 1 is dissolved ever since the lowest polytomy prior is applied both under the polytomy and resolution classes (Supplementary Table 4).

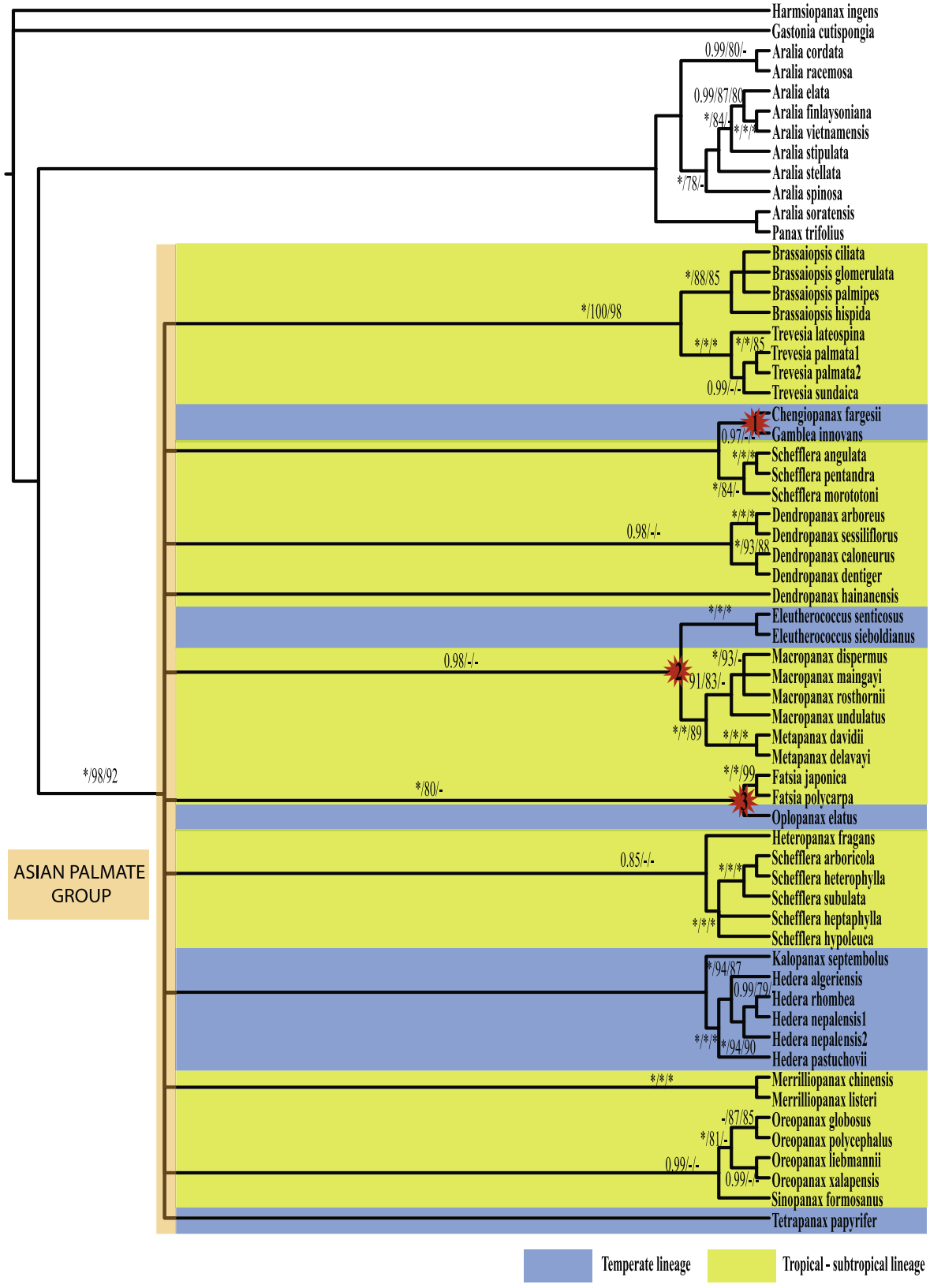

Fig. 2. Majority rule consensus tree obtained from the *nr*ITS Bayesian Inference analysis of the Asian Palmate group. Branch support is provided above branches as follows: PP values from the BI, followed by BSs from ML and MP analyses. Asterisks indicate branch supports = 1.00 PP or 100% BS. Hyphens indicate <0.95 PP or <75% BS from ML or MP. Incongruent nodes between the ITS and plastid reconstructions are numbered.

Likelihood convergence is soon achieved in the plastid resolvability analyses. However, topological convergence was not achieved even when using 3×10^5 cycles, therefore these results should be taken with caution. The incongruent nodes 1a and1b

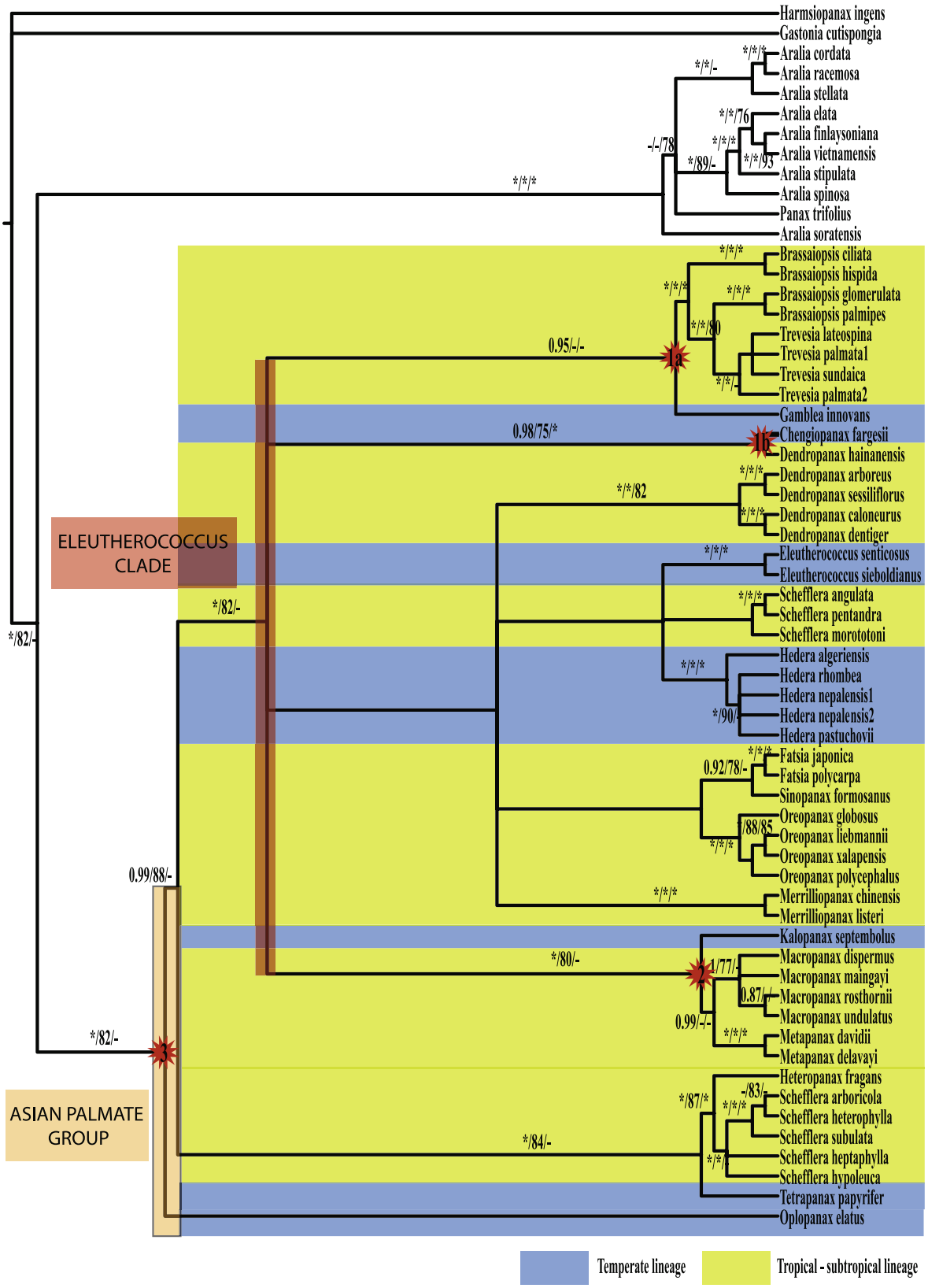

Fig. 3. Majority rule consensus tree obtained from the five-plastid (*atp*B-*rbc*L, *psb*A-*trn*H, *trn*L-*trn*F, *nadh*F, *rpL*16, and *rpS*16) Bayesian Inference analysis of the Asian Palmate group. Branch support is provided above branches as follows: PP values from the BI, followed by BSs from ML and MP analyses. Asterisks indicate branch supports = 1.00 PP or 100% BS from ML or MP. Hyphens indicate <0.95 PP or <75 BS from ML or MP. Incongruent nodes between the ITS and plastid reconstructions are numbered.

(Fig. 3) are dissolved both under the polytomy and resolution class analyses (Supplementary Table 4). The node 2 (Fig. 3) is highly supported in the polytomy class analyses while dissolved in the resolution class ones (Supplementary Table 4). On the

other hand, node 3 (Fig. 3) is highly supported in all the polytomy resolvability analyses except when the resolution class prior is conducted under the highest tree prior (Supplementary Table 4).

3.4. Hypothesis testing of the sister-groups of Hedera

The ITS Bayes Factors recover very strong evidence against the unconstrained topology when compared to all the alternative topologies, being the most favored ones the *Trevesia-Brassaiopsis* group and *Dendropanax* subgen. *Textoria pro parte* (Supplementary Table 5). On the other hand, the sister-group relationship between *Hedera* and *Eleutherococcus* or the neotropical *Schefflera*s is the only one significantly rejected with the AU test when using the ITS dataset, although with marginal support (Supplementary Table 5). The plastid Bayes Factors recovered very strong evidence in favor to three of the competing sister-group hypotheses of *Hedera*: the *Trevesia-Brassaiopsis* group, *Dendropanax* subgen. *Textoria pro parte*, and *Merrilliopanax* (Supplementary Table 5), whereas very strong evidence against *Kalopanax* (Supplementary Table 5). On the other hand, the plastid AU test rejects *Kalopanax*, the *Trevesia-Brassaiopsis* group and *Dendropanax* subgen. *Textoria pro parte* as sisters to *Hedera* (Supplementary Table 5).

3.5. Divergence age estimates

Results from the unconstrained ITS age estimates (BEAST) reveal 20 myr (HDP 11–31 myr, Table 2, and Fig. 4) for the crown of *Hedera*. Since no sister is recovered for *Hedera*, no stem age can be extracted with certainty. Results from the constrained ITS age estimates (MCMCtree) reveal a stem age for *Hedera* that varies from 53 myr (HDP 42–66 myr) to 62 myr (HDP 47–72 myr) depending on the constrained topology used as input tree (Table 2, and Fig. 4). Results from the unconstrained plastid age estimates indicate 73 myr (HDP 55–98 myr, Table 2, and Fig. 4) for the crown of the Asian Palmate group and 8 myr (HDP 2–17 myr, Table 2 and Fig. 4) for the crown of *Hedera*. No stem age is retrieved with confidence since no sister-group is recovered for *Hedera*. The ages recover for the stem age of *Hedera* based on the constrained plastid analyses vary between 34 myr (HDP 26–51 myr) and 40 myr (HDP 28–59 myr) depending on the constrained input tree (Table 2, and Fig. 4). The ITS age estimates for the stem of *Hedera* are one and a half higher than the ones recovered with the plastid dataset (Table 2, and Fig. 4). The ITS estimates for the crown of *Hedera* reveal an age from more than twice to more than four times higher than the ones obtained in the plastid reconstruction (Table 2, and Fig. 4). The ITS posterior distributions are consistently from one and a half to twice higher than in the plastid ones (Table 2).

4. Discussion

4.1. Topological incongruence in the Asian Palmate group

The present study reveals different phylogenetic histories for the Asian Palmate group as inferred from the significant discordancy detected between the nuclear ITS and plastid reconstructions. This Asian Palmate discordance may become negligible at the family-level phylogeny, which may explain why genome incongruence has never been reported before for the Araliaceae (Mitchell et al., 2012; Plunkett et al., 2004). Our findings on the Asian Palmate incongruence add a new level of complexity but provide interesting information for the interpretation of the origin and early evolution of this group. The independent analysis of the *nr*ITS and plastid datasets allowed us to uncover two processes that may have operated simultaneously: early radiation and inter-lineage hybridization, hindering the recovery of unequivocal phylogenetic signals.

Incongruence between gene trees may be indicative of biological processes in ancestral species or along the evolutionary lines that connect ancestral species with descendants (such as incomplete lineage sorting, horizontal gene transfer, gene duplication, recombination, or hybridization; Degnan and Rosenberg, 2009; Rannala and Yang, 2008). On the other hand, methodological artifacts derived from sampling errors, long-branch attraction or undetected paralog genes may also produce topological discordances (Degnan and Rosenberg, 2009). Incongruence between gene trees ultimately poses the question of which one is the gene tree that better reflects the species tree. In our particular case, sampling error seems unlikely as determinant for the genomes incongruence because high PP (>0.95) or BS (>70%) values support the incongruent clades in both phylogenies (Figs. 1 and 3). High levels of support coming from bootstrapping and posterior distributions are used as assessment of robustness (Huson and Bryant, 2006) indicating no sampling error if the incongruent clades are highly supported (Pelser et al., 2010). The fact that all the incongruent clades except for three (Supplementary Table 4) are supported with both high PP and BS values suggests confidence in them (Alfaro and Holder, 2006). Moreover, high support for incongruent clades persists even in the polytomy resolvability analyses except for two that are consistently dissolved when using the plastid dataset (Supplementary Table 4). Long-branch attraction can also be discarded since the nuclear and plastid reconstructions obtained after removing long branches (*Tetrapanax* and *Oplopanax*) depicted the same level of incongruence between genome reconstructions. However, it is possible that the presence of undetected paralogous genes may be causing the incongruence detected. A process of ancient hybridization followed by erratic recombination may partially explain the detected incongruent pattern underlying the ITS large basal polytomy (Álvarez and Wendel, 2003; Hughes et al., 2006; Nieto Feliner and Roselló, 2007). Ancient polyploidization events seem to have been involved either in the origin of the Asian Palmate group or in the evolution of all the main different lineages (Yi et al., 2004). If these poliploidizations resulted from an early inter-lineage hybridization it is then possible that biased concerted evolution may have erased the trace of the hybridization in the ITS sequences resulting in an incongruent pattern when compared to the plastid one.

Incomplete lineage sorting is an important source for incongruence unlikely to happen in deep phylogenies (Degnan and

Table 2
Summary of the divergence times obtained in the topologically unconstrained BEAST analyses and in MCMCtree analyses of the four constrained topologies. Mean and 95% confidence intervals obtained from plastid and ITS age estimates are provided for two nodes (stem and crown of *Hedera*). The Asian Palmate crown estimates are only provided from plastid reconstructions, since this node was age-calibrated in the ITS estimates. The crown ages of the *Eleutherococcus* clade are only provided for plastid reconstructions since this node is not recovered in the ITS analyses.

Input tree topology	Asian Palmate crown *Plastid*	Eleutherococcus clade crown *Plastid*	*Hedera* stem *Plastid*	*ITS*	*Hedera* crown *Plastid*	*ITS*
Unconstrained	72.55 (55–98)	56.47 (47–72)	36.6	51.55	7.65 (2–17)	20.4 (11–31)
(*Hedera, Kalopanax*)	67.6 (52–91)	54 (45–73)	34.3 (26–51)	54.5 (37–69)	7.1 (2–16)	31.1 (12–51)
(*Hedera, Eleutherococcus, Neotropical Schefflera*)	70.1 (54–95)	58 (47–79)	40.1 (28–59)	62.2 (49–71)	7.5 (2–18)	31.3 (11–53)
(*Hedera, Dendropanax subgen. Textoria pro parte*)	69.9 (54–95)	58 (47–80)	37.6 (26–56)	61.9 (47–72)	7.4 (2–17)	31.1 (11–53)
(*Hedera, Trevesia-Brassaiopsis*)	68.1 (54–88)	56.3 (48–72)	39.7 (31–55)	53.3 (42–66)	8.4 (3–18)	22.3 (13–35)

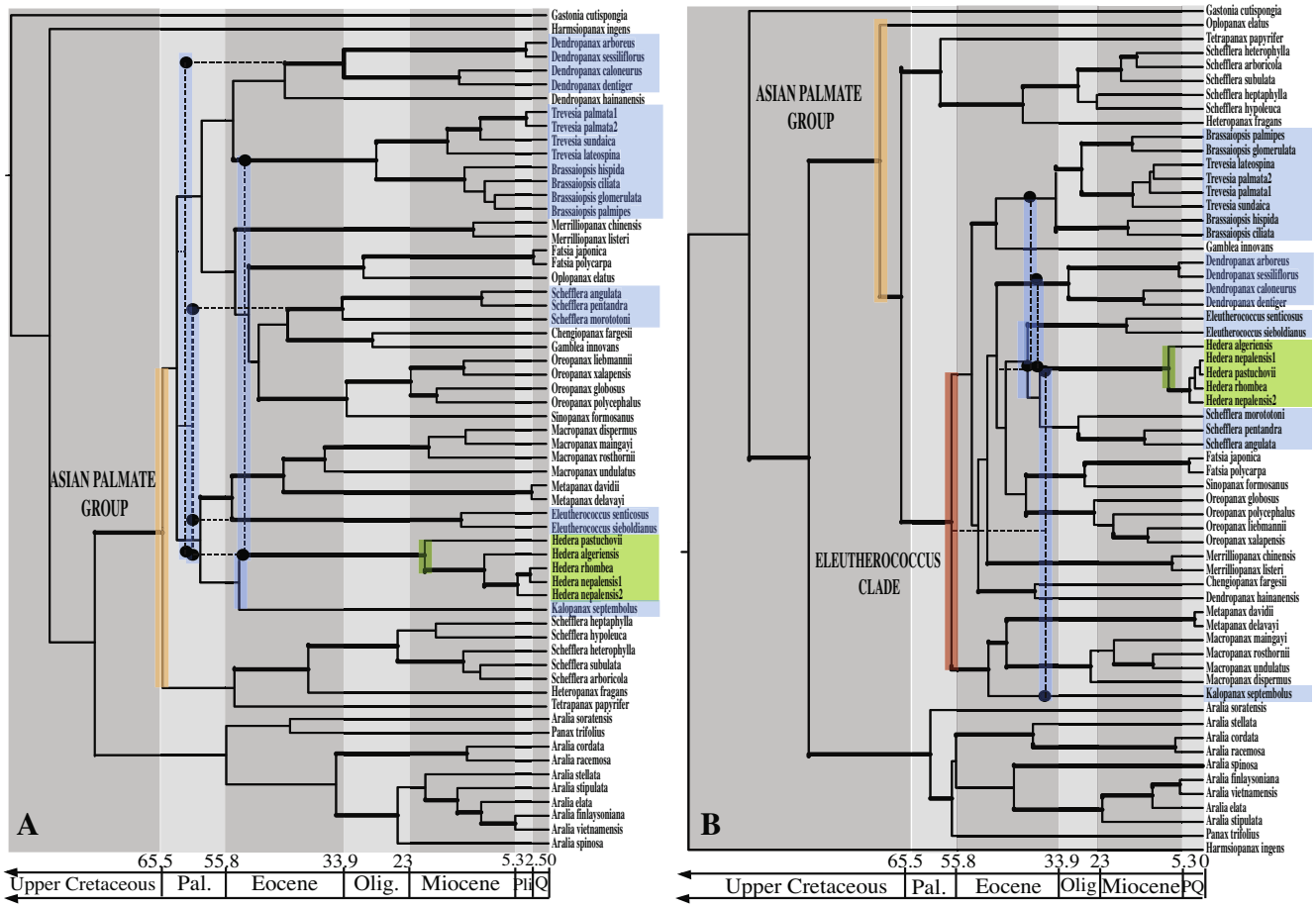

Fig. 4. Chronograms obtained in BEAST from the unscontrained analyses of the Asian Palmate group. Thick lines indicate branches with statistical support in the phylogenetic analyses ($\geqslant$0.95 PP from BI, and/or $\geqslant$75% BS from MP and/or ML). Dashed lines represent the age of divergence of the stem of *Hedera* estimated in the constrained MCMCTREE analyses. The lineage of *Hedera* is highlighted in green and the alternative sister-groups are highlighted in blue. Abbreviations: "Pal" refers to the Paleocene, "Olig" to the Oligocene, "Pli" to the Pliocene, "Q" to the Quaternary, and "PQ" to the Pliocene-Quaternary periods. (A) Chronogram obtained from the analysis of the *nr*ITS dataset. (B) Chronogram obtained from the analysis of the plastid dataset (*atp*B-*rbc*L, *psb*A-*trn*H, *trn*L-*trn*F, *nadh*F, *rpL*16, and *rpS*16).

Rosenberg, 2009). However, it may become highly probable if an early radiation occurred (Degnan and Rosenberg, 2009). This is simply because persistence of multiple gene lineages through short internal branches may produce ancient coalescent events leading to discordant relationships between the external nodes (Degnan and Rosenberg, 2009). The genome incongruence detected for the Asian Palmate group may reflect an incomplete lineage sorting pattern derived from an ancient radiation since few of the total informative sites are synapomorphies between genera (21% in ITS and 17% in the plastid matrix). This is interpreted as an evidence of short deep branches rather than scarcity of informative characters since the overall number of informative sites between genera (190) is similar to the one obtained for other well-resolved clades of Araliaceae that are comparable in the number of genus-level lineages (i.e. 221 for *Polyscias*/*Pseudopanax* clade extracted from Mitchell et al., 2012). Therefore, the incongruence detected may be due to ancient coalescent events. Additionally, ancient interlineage hybridization can be underlying the genome discordances detected in the Asian Palmate group resulting in a phylogenetic pattern similar to the one produced by the incomplete lineage sorting. This, together with the possible biased concerted evolution process already discussed for the ITS sequences may well explain both the genomes incongruence and the scarcity of internal resolution independently recovered in both phylogenies. Besides, the probability that the most common gene tree topology recovered may differ from the species tree becomes very high in short deep-branched topologies if the underlying species tree is asymmetrical (Rannala and Yang, 2008). Species tree asymmetry is suggested for the Asian Palmate group in the plastid reconstructions and recovered in the species tree suggesting possible inconsistency of the phylogenetic methods as an additional source of incongruence.

The origin of the Asian Palmate group seems to be Asia as inferred from the ancestral area reconstruction performed by Mitchell et al. (2012). Our divergence age estimates place the crown of the Asian Palmate group in the Upper Cretaceous–Paleocene transition (Fig. 4), consistent with the results in Mitchell et al. (2012). At the beginning of the Upper Cretaceous the E Asian volcanic belt created a montane and temperate climate (Kirillova, 2011), which contributed to stress the Upper Cretaceous general cooling particularly in Asia (Lim and Lee, 2005; Okudaira et al., 2001). It seems then plausible that the new environments produced during the Upper Cretaceous cooling may have promoted a rapid diversification of cool-tolerant lineages in the early divergence of the Asian Palmate group. Indeed, all the temperate genera are involved in the large basal polytomies recovered for the early differentiation of the group. Interestingly, the Upper Cretaceous–Paleocene has also been reported as the temporal framework for the early divergence of other temperate plant genera in Asia from their tropical counterparts (e.g., 60 mya (46–70) for *Acer*/*Dipteronia*, Renner et al., 2008; 62 mya (58–63) for *Aesculus*, Harris et al., 2009). The early and fast lineage diversification of the Asian Palmate group

may have been reinforced by inter-lineage hybridization and polyploidization. Indeed, (1) cool periods have been seen as an opportunity to lineage admixture resulting in genome doublings to restore fertility in the hybrids (Stebbins, 1984), (2) all the Asian Palmate genera are polyploids (Yi et al., 2004), and (3) all the major genome incongruence detected are due to the placement of temperate genera. This early inter-lineage hybridization hypothesis seems plausible since not only genetic compatibility of artificial inter-generic hybrids have been demonstrated in Araliaceae (Knobloch, 1972), but ancestral intergeneric hybridization has been recently suggested as a possible explanation for the 100% ITS2 sequence identity between *Eleutherococcus* and *Panax* (Song et al., 2012). Rising of mountain ranges has been seen as providing historical corridors between areas allowing temperate lineages to reach tropical regions (Sánchez Meseguer et al., 2013). In our particular case, the Upper Cretaceous E Asian mountain uplift may have also acted as a corridor making lineages contact possible. A similar scenario has been proposed for a South American orchid genus where an early radiation coupled with allopolyploidizations has been detected and linked to the cooling occurred during the middle/late Miocene (Antonelli et al., 2010). However, further studies are needed to investigate into this new evolutionary scenario for the origin and early diversification of the Asian Palmate group.

4.2. Origin and early differentiation of the Hedera lineage

Despite the extensive set of exhaustive analyses carried out in the present work and the number of molecular regions analyzed, the sister-group of *Hedera* could not be recovered robustly. We not only could not reject any of the alternative sisters previously suggested, but also we added new possible ones (*Eleutherococcus* and the Neotropical *Schefflera*) that do not fit any of the three *Hedera's* sister-group hypotheses under evaluation (tropical conservatism, phylogenetic niche conservatism, radiation). Moreover, the divergence time estimates provide similar timeframes compatible with all the evaluated scenarios.

The lack of *Hedera* resolution in the plastid tree is due to the few (two) and incongruent synapomorphies detected between *Hedera* and other genus-level lineages. Sampling error seems unlikely since the overall number of between genus-lineage synapomorphies is high (33). The first alternative explanation is that the divergence between the lineage of *Hedera* and its sister may have taken place soon after its ancestor, preventing it from accumulating synapomorphies between sister lineages. The second alternative explanation draws the opposite scenario with the divergence between the lineage of *Hedera* and its sister long after its ancestor, combined with a slow substitution rate. Irrespective of the genome and constrained topology used, the stem posterior distribution recovered for *Hedera* overlapped those found for the crown of the *Eleutherococcus* clade and even for the Asian Palmate group (Table 2). It then seems plausible to place the divergence of the lineage of *Hedera* from its sister early at the origin of the *Eleutherococcus clade* or the Asian Palmate group, which suggests a better fit with the first alternative explanation. Accordingly, the lineage of *Hedera* may have also been involved in the early radiation with lineage admixture already proposed for the Asian Palmate group. Interestingly, genetic compatibility of artificial inter-generic hybrids has been particularly demonstrated between *Hedera* and *Fatsia* (i.e., *Fatshedera*; Knobloch, 1972). This deep hybrid scenario allows conciliation of the two incongruent phylogenetic histories. We propose that a combination of the niche conservatism and radiation hypotheses is the most probable scenario for the origin of the *Hedera* lineage. Indeed, (1) half of the incongruent between-genera synapomorphies linked *Hedera* with other temperate genera of the Asian Palmate group while none with the morphologically similar genera; and (2) the early divergence of the lineage of *Hedera* was involved in the early radiation and inter-lineage hybridization of the Asian Palmate group.

Long time isolation seems to have affected the lineage of *Hedera* as inferred from the: (1) extended time between the putative stems and crown (24(17)–39(41) myr) and (2) high number of synapomorphies, which is among the highest of the Asian Palmate group. A long time between the divergence of the stem and crown of *Hedera* is congruent with previous evolutionary hypotheses that suggested an old origin for the genus (Cretaceous, Pojarkova, 1951; Oligocene, Rim, 1994) but recent diversification of the extant species (Ackerfield and Wen, 2003; Pojarkova, 1951; Valcárcel and Vargas, 2013). Indeed, previous authors (Pojarkova, 1951; Valcárcel et al., 2003) proposed an alternation of periods of inter-continental range expansion and reduction coupled with extinction and speciation processes. This biogeographic scenario can only be envisage if long time has lasted between the early diversification of the extant species of *Hedera* and its stem. Besides, the age of the stem of *Hedera* recovered from posterior distributions are congruent with the fossil data used to support the above-described biogeographic hypothesis. On the one hand, plastid estimates place the origin of the lineage back to the Eocene–Oligocene, which is congruent with the oldest reliable fossil of *Hedera* (Oligocene, Rim, 1994). On the other hand, the ITS estimates give the Upper Cretaceous–Paleocene, suggesting a much older scenario congruent with the one proposed by Pojarkova (1951). However, the reliability of the fossils used by Pojarkova (1951) has never been evaluated. Besides, ITS estimates should be taken with caution because of the huge uncertainty associated and the issues already explained for the ITS evolution in the Asian Palmate group.

Our divergence estimates suggest the late Miocene (plastid reconstruction) or the Oligocene (ITS reconstruction) as the temporal context for the early divergence of the extant species of *Hedera,* which has been placed in the Mediterranean basin (Valcárcel and Vargas, 2013). The Messinian age recovered from the plastid dataset is congruent with the Mediterranean fossil record since the first reliable fossil of *Hedera* in Europe dates from the Miocene in the Iberian Peninsula (11.61 ± 0.05–5.33 ± 0.05 mya; Muller, 1981). *Hedera* is a thermophilic genus (Andergassen and Bauer, 2002; Parker, 1962) that has been used as climate-indicator for warm periods (late Eocene: Axelrod, 1975; Oligocene: Kong, 2000; Rim, 1994; Miocene–Pliocene: Kovar-Eder et al., 2006; mid Holocene: Bottema, 2001; Iversen, 1944; late Holocene: Müller et al., 2005; Eeminan: Andersen, 1965). Indeed, ivies are considered as part of the dry sub-tropical Tertiary flora (Axelrod, 1975; Herrera, 1992; Verdú et al., 2003) that dominated the Mediterranean basin vegetation during the Miocene prior to the Messinian Salinity Crisis (6.9–6.6 mya, Krijgsman et al., 1999). It is therefore difficult to envisage the origin of the recent divergence of *Hedera* in a late Miocene Mediterranean context where the temperature and aridity increases lead to the extinction of most of the sub-tropical Tertiary lineages (Jiménez-Moreno et al., 2010). However, it is possible that *Hedera* speciation increased during the Messinian Salinity Crisis as a result from its geographic isolation in distant humid refugia in the Mediterranean basin, as suggested for other Mediterranean plants (Lo Presti and Oberprieler, 2009). Recent studies have questioned the common interpretation of speciation rate increase from cladogenesis proliferation events in phylogenies since this may also be the result of a mass extinction event or a previous period of rate stasis (Crisp and Cook, 2009; Fiz-Palacios and Valcárcel, 2013; Stadler, 2011). Sampling incompleteness within *Hedera* prevented us from conducting the proper analyses to evaluate these scenarios. However, it would be interesting to investigate whether the origin of the extant species of *Hedera* was due to a mass extinction event at the Messinian, a previous rate stasis followed by an extinction rate decrease or a true speciation rate increase coinciding with the Messinian (see above). A mass extinction scenario

caused by the climate change occurred at the Messinian would be likely for ivies given their niche preferences. On the other hand, the rate stasis scenario also seems likely since the progressive development of the Mediterranean climate, already underway in the Late Miocene (Suc, 1984), may have provided a suitable climate for *Hedera* after the Messinian salinity crisis reduced its extinction rate.

5. Conclusions

The independent analysis of the nuclear and plastid phylogenies forced by the discordance detected, provided the key to the re-interpretation of the large basal polytomy of the Asian Palmate group as the biological footprint of an early radiation and to uncover a parallel lineage admixture. The early radiation took placed in Asia under the general cooling of the Upper Cretaceous and the East Asia mountain uplift, which may have produced new temperate environments and corridors allowing lineages connection. We hypothesized that the divergence of the *Hedera* linage, and the remaining temperate lineages of the Asian Palmate group, was driven by Upper Cretaceous cooling since they all were involved in the early radiation. Therefore, the combination of a radiation with lineage admixture prevented us from disclosing the closest relatives of *Hedera*. However, we provide meaningful insights for future studies into the origin and early diversification of this long isolated genus, that are consistent with the history described for the early differentiation of other temperate plant lineages from their tropical counterparts.

Acknowledgments

The authors thank two anonymous reviewers as well as H.A. McAllister and P. Vargas for their generous discussion and meaningful comments on the manuscript, A. Mitchell and R. Li for kindly providing the DNA matrix used in Mitchell et al. (2012), M. Mazuecos and N. García Medina for advise on maps, S. Martín-Bravo for the picture of *Hedera iberica* used for the graphical abstract, and staff of the Laboratory of Analytical Biology at the National Museum of Natural History of the Smithsonian Institution for technical assistance. This work was partially supported by a grant to V. Valcárcel from Junta de Andalucía.

Appendix A. Supplementary material

Supplementary data associated with this article can be found, in the online version, at http://dx.doi.org/10.1016/j.ympev.2013.10.016.

References

Ackerfield, J., 2001. Trichome morphology in *Hedera* (Araliaceae). Edinb. J. Bot. 58, 259–267.
Ackerfield, J., Wen, J., 2003. Evolution of *Hedera* (the ivy genus, Araliaceae): Insights from chloroplast DNA data. Int. J. Plant Sci. 164, 593–602.
Alfaro, M.E., Holder, M.T., 2006. The posterior and the prior in Bayesian phylogenetics. Annu. Rev. Ecol. Evol. Syst. 37, 19–42.
Álvarez, I., Wendel, J.F., 2003. Ribosomal ITS sequences and plant phylogenetic inference. Mol. Phylogenet. Evol. 29, 417–434.
Andergassen, S., Bauer, H., 2002. Frost hardiness in the juvenile and adult life phase of ivy (*Hedera helix* L.). Plant Ecol. 161, 207–213.
Andersen, S.T., 1965. Interglacialer og interstadialer i Danmarks Kvartær. Meddelelser Fra Dansk Geologisk Forening 15, 486–506.
Antonelli, A., Verola, C.F., Parisod, C., Lovisa, A., Gustafsson, S., 2010. Climate cooling promoted the expansion and radiation of a threatened group of South American orchids (Epidendroideae: Laeliinae). Biol. J. Linn. Soc. Lond. 100, 597–607.
Axelrod, D., 1975. Evolution and biogeography of Madrean-Tethyan sclerophyll vegetation. Ann. Mo. Bot. Gard. 62, 280–334.
Bergsten, J., Nilsson, A.N., Ronquist, F., 2013. Bayesian test topology hypotheses with an example from Diving Beetles. Syst. Biol. 62, 660–673.
Bottema, S., 2001. A note on the pollen representation of ivy (*Hedera helix* L.). Rev. Palaeobot. Palynol. 117, 159–166.
Calestani, V., 1905. Contributo alla sistematica delle Ombrellifere d'Europa. Webbia 1, 89–280.
Chandler, G.T., Plunkett, G.M., 2004. Evolution in Apiales: nuclear and chloroplast markers together in (almost) perfect harmony. Bot. J. Linn. Soc. 144, 123–147.
Crisp, M.D., Cook, L.G., 2009. Explosive radiation or cryptic mass extinction? Interpreting signatures in molecular phylogenies. Evolution 63, 2257–2265.
Degnan, J.H., Rosenberg, N.A., 2006. Discordance of species trees with their most likely gene trees. PLoS Genet. 2, 762–768.
Degnan, J.H., Rosenberg, N.A., 2009. Gene tree discordance, phylogenetic inference and multispecies coalescence. Trends Ecol. Evol. 24, 332–340.
Doweld, A., 2001. Prosyllabus tracheophytorum, tentamen systematis plantarum vascularium (Tracheophyta) (An attempted system of the vascular plants). Pensoft, Moscow.
Drummond, A.J., Rambaut, A., 2007. BEAST: Bayesian evolutionary analysis by sampling trees. BMC Evol. Biol. 7, 214.
Edgar, R.C., 2004. MUSCLE: multiple sequence alignment with high accuracy and high throughput. Nucl. Acids Res. 32, 1792–1979.
Fiaschi, P., Plunkett, G.M., 2011. Monophyly and phylogenetic relationships of Neotropical Schefflera (Araliaceae) based on plastid and nuclear markers. Syst. Bot. 36, 806–817.
Fiz-Palacios, O., Valcárcel, V., 2013. From Messinian crisis to Mediterranean climate: a temporal gap of diversification recovered from multiple plant phylogenies. Perspect. Plant Ecol. Evol. Syst. 15, 130–137.
Frodin, D.G., Govaerts, R., 2003. World check-list and bibliography of Araliaceae. The Royal Botanical Gardens, Kew.
Goloboff, P., Farris, J., Nixon, K., 2003. T.N.T. tree anlysis using new tecnologies. <http://www.zmuc.dk/public/phylogeny/tnt>.
Green, A.F., Ramsey, T.S., Ramsey, J., 2011. Phylogeny and Biogeography of Ivies (*Hedera* spp., Araliaceae), a polyploid complex of woody vines. Syst. Bot. 36, 1114–1127.
Harms, H., 1898. Araliaceae. In: Engler, A., Prantl, K. (Eds.), Die natürlichen Pflanzenfamilien, vol. III. Verlag von Wilhelm Engelmann, Leipzig, pp. 1–62.
Harris, A.J., Xiang, Q.Y., Thomas, D.T., 2009. Phylogeny, origin, and biogeographic history of *Aesculus* L. (Sapindales) – an update from combined analysis of DNA sequences, morphology and fossils. Taxon 58, 1–19.
Heled, J., Drummond, A.J., 2010. Bayesian inference of species trees from multilocus data. Mol. Biol. Evol. 27, 570–580.
Herrera, C., 1992. Historical effects and sorting processes as explanations for contemporary ecological patterns: character syndromes in Mediterranean woody plants. Am. Nat. 140, 421–446.
Hipp, A.L., Hall, J.C., Sytsma, K.J., 2004. Congruence versus phylogenetic accuracy: revisiting the incongruence length difference test. Syst. Biol. 53, 81–89.
Huelsenbeck, J.P., Ronquist, F., 2001. MRBAYES: Bayesian inference of phylogenetic trees. Bioinformatics 17, 754–755.
Hughes, C.E., Eastwood, R.J., Bailey, C.D., 2006. From famine to feast? Selecting nuclear DNA sequence loci for plant species-level phylogeny reconstruction. *Philos*. Trans. Roy. Soc. Lond. B Biol. Sci. 361, 211–225.
Hurvich, C.M., Tsai, C.L., 1989. Regression and time series model selection in small samples. Biometrika 76, 297–307.
Huson, D.H., Bryant, D., 2006. Application of phylogenetic networks in evolutionary studies. Mol. Biol. Evol. 23, 254–267.
Iversen, J., 1944. Viscum, Hedera and Ilex as climate indicators. Geol. Fören. Stockholm Foörh. 66, 463–483.
Jiménez-Moreno, G., Fauquette, S., Suc, J.P., 2010. Miocene to Pliocene vegetation reconstruction and climate estimates in the Iberian Peninsula from pollen data. Rev. Paleobot. Palynol. 162, 410–415.
Jobb, G., 2007. TREEFINDER version of February 2007. Munich, Germany. Distributed by the author at <www.treefinder.de> (Last accessed 12.12).
Jobb, G., Haeseler, A., Strimmer, K., 2004. TREEFINDER: a powerful graphical analysis environment for molecular phylogenetics. BMC Evol. Biol. 4, 18.
Kass, R.E., Raferty, A.E., 1995. Bayes factors. J. Am. Stat. Assoc. 90, 773–795.
Kirillova, G.L., 2011. The Cretaceous of the East Asian continental margin: Stratigraphy, paleogeography, and paleoclimate. The Island Arc 20, 57–77.
Knobloch, I.W., 1972. Intergeneric hybridization in flowering plants. Taxon 21, 97–103.
Kong, W.S., 2000. Vegetational history of the Korean Peninsula. Glob. Ecol. Biogeogr. 9, 391–402.
Kovar-Eder, J., Kvacek, Z., Martinetto, E., Roiron, P., 2006. Late Miocene to Early Pliocene vegetation of southern Europe (7–4Ma) as reflected in the megafossil plant record. Palaeogeogr. Palaeoclimatol. Palaeoecol. 238, 321–339.
Krijgsman, W., Hilgen, F.J., Raffi, I., Sierro, F.J., Wilson, D.S., 1999. Chronology, causes and progression of the Messinian salinity crisis. Lett. Nat. 400, 652–655.
Lewis, P.O., Holder, M.T., Holsinger, K.E., 2005. Polytomies and Bayesian phylogenetic inference. Syst. Biol. 54, 241–253.
Lewis P.O., Holder, M.T., Swofford, D., 2010. Phycas 1.2.0 user manual. Distributed by the authors. Available from: <http://hydrodictyon.eeb.uconn.edu/projects/phycas/index.php/Phycas> Home. [Last accessed: December 2012].
Li, R., Wen, J., 2013. Phylogeny and biogeography of *Dendropanax* (Araliaceae), an Amphi-Pacific Disjunct Genus between Tropical/Subtropical Asia and the Neotropics. Syst. Bot. 38, 536–551.

Lim, H.S., Lee, Y., 2005. Cooling history of the Upper Cretaceous Palgongsan Granite, Gyeongsang Basin, SE Korea and its tectonic implication for uplift on the active continental margin. Tectonophysics 403, 151–165.
Lo Presti, R.M., Oberprieler, Ch., 2009. Evolutionary history, biogeography and eco-climatological differentiation of the genus *Anthemis* L., (Compositae, Anthemideae) in the Circum-Mediterranean area. J. Biogeogr. 36, 1313–1332.
Lowry II, P.P., Plunkett, G.M., Wen, J., 2001. Generic relationships in Araliaceae: looking into de crystal ball. South Afr. J. Bot. 70, 382–392.
Lum, C., Maze, J., 1989. A multivariate analysis of the trichomes of *Hedera* L.. Watsonia 17, 409–418.
Maddison, W.P., Maddison, D.R., 2011. Mesquite: a modular system for evolutionary analysis. Version 2.74. 2011. Available from: <www.mesquiteproject.org> (Last accessed 09.12).
Manchester, S.R., 1994. Fruits and seeds of the middle Eocene Nut Beds Flora, Clarno Formation, Oregon. Palaeontogr. Am. 58, 38–39.
McAllister, H.A., Rutherford, A., 1990. *Hedera helix* L. and *H. hibernica* (Kirchner) Bean (Araliaceae) in the British Isles. Watsonia 18, 7–15.
Mickevich, M.F., Farris, S.J., 1981. The implications of congruence in Menidia. Syst. Zool. 30, 351–370.
Mitchell, A., Wen, J., 2004. Phylogeny of the Asian core Araliaceae clade based on Granule-Bound Starch Synthase I (GBSSI) sequence data. Taxon 53, 29–41.
Mitchell, A., Wen, J., 2005. Phylogeny of *Brassaiopsis* (Araliaceae) in Asia based on nuclear ITS and 5S-NTS DNA sequences. Syst. Biol. 30, 872–886.
Mitchell, A., Li, R., Brown, J.W., Schönberger, I., Wen, J., 2012. Ancient divergence and biogeography of *Raukaua* (Araliaceae) and close relatives in the southern hemisphere. Aust. Syst. Bot. 25, 432–446.
Müller, J., 1981. Fossil pollen records of extant angiosperms. Bot. Rev. 47, 1–142.
Müller, U.C., Klotz, S., Geyh, M.A., Pross, J., Bond, G.C., 2005. Cyclic climate fluctuations during the last interglacial in central Europe. Geology 33, 449–452.
Nagy, L.G., Házi, J., Szappanos, B., Kocsubé, S., Balint, B., Rákhelym, G., Vágvölgyi, C., Papp, T., 2012. The Evolution of defense mechanisms correlate with the explosive diversification of autodigesting *Coprinellus* Mushrooms (Agaricales, Fungi). Syst. Biol. 61, 1–13.
Nieto Feliner, G., Roselló, J.A., 2007. Better the devil you know? Guidelines for insightful utilization of *nr*DNA ITS in species-level evolutionary studies in plants. Mol. Phylogenet. Evol. 44, 911–919.
Okudaira, T., Hayasaka, Y., Himeno, O., Watanabe, K., Sakurai, Y., Ohtomo, Y., 2001. Cooling and inferred exhumation history of the Ryoke metamorphic belt in the Yanai district, south-west Japan: Constraints from Rb–Sr and fission-track ages of gneissose granitoid and numerical modeling. Island Arc 10, 98–115.
Parker, J., 1962. Relationships among cold hardiness, water-soluble protein, anthocyanins, and free sugars in *Hedera helix* L.. Plant Physiol. 37, 809–813.
Pelser, P.B., Kennedy, A.H., Tepe, E.J., Shidler, J.B., Nordensta, B., Kadereit, J.W., Watson, L.E., 2010. Patterns and causes of ncongruence between plastid and nuclear Senecioneae (Asteraceae) phylogenies. Am. J. Bot. 91, 856–873.
Planet, P.J., 2006. Tree disagreement: measuring and testing incongruence in phylogenies. J. Biomed. Inform. 39, 86–102.
Plunkett, G.M., Lowry II, P.P., 2001. Relationships among "Ancient Araliads" and their significance for the systematics of Apiales. Mol. Phylogenet. Evol. 19, 259–276.
Plunkett, G.M., Wen, J., Lowry II, P.P., 2004. Infrafamilial classifications and characters in Araliaceae: Insights from the phylogenetic analysis of nuclear (ITS) and plastid (*trnL-trn*F) sequence data. Plant Syst. Evol. 245, 1–39.
Plunkett, G.M., Lowry II, P.P., Frodin, D.G., Wen, J., 2005. Phylogeny and geography of *Schefflera*: pervasive polyphyly in the largest genus of Araliaceae. Ann. Mo. Bot. Gard. 92, 202–224.
Pojarkova, A.I., 1951. The chinese species of ivy and their taxonomic and geographic connections. Natulae Systematicae ex Herbario Botanici nomine V.L. Komarovii Academiae Scientiarum URSS XIV, 224–264.
Posada, D., 2008. JModelTest: phylogenetic model averaging. Mol. Biol. Evol. 25, 1253–1256.
Posada, D., Buckley, T.R., 2004. Model selection and model averaging in phylogenetics: Advantages of Akaike Information Criterion and Bayesian approaches over Likelihood Ratio Tests. Syst. Biol. 53, 793–808.
Rambaut, A., Drummond, A.J., 2007. Tracer v1.4. http://beast.bio.ed.ac.uk/Tracer (Last accessed 2012).
Rannala, B., Yang, Z., 2007. Inferring speciation times under an episodic molecular clock. Syst. Biol. 56, 453–466.
Rannala, B., Yang, Z., 2008. Phylogenetic inference using whole genomes. Annu. Rev. Genomics Hum. Genet. 9, 217–231.
Renner, S., Grimm, G.W., Schneeweiss, G.M., Stuessy, T.F., Ricklefs, R.E., 2008. Rooting and dating Maples (*Acer*) with an uncorrelated-rates molecular clock: Implications for North American/Asian Disjunctions. Syst. Biol. 57, 795–808.
Rim, K.H., 1994. Fossils of North Korea. Science and Technology Press, Pyongyang.
Ronquist, F., Huelsenbeck, J.P., Teslenko, M., 2011. Draft MrBayes version 3.2 manual: Tutorial and model summaries. <http://mrbayes.sourceforge.net/mb3.2_manual.pdf> (Last accessed 09.13].
Ronquist, F., Teslenko, M., van der Mark, P., Ayres, D.L., Darling, A., Höhna, S., Larget, B., Liu, L., Suchard, M.A., Huelsenbeck, J.P., 2012. MrBayes 3.2: efficient bayesian phylogenetic inference and model choice across a large model space. Syst. Biol. 61, 539–542.
Sánchez Meseguer, A., Aldasoro, J., Snamartín, I., 2013. Bayesian inference phylogeny and range evolution reveals a complex evolutionary history in St. John's wort (*Hypericum*). Mol. Phylogenet. Evol. 67, 379–403.
Seemann, B., 1868. Revision of the Natural Order Hederaceae. L. Reeve and Co., London.
Shimodaira, H., 2002. An approximately unbiased test of phylogenetic tree selection. Syst. Biol. 51, 492–508.
Song, J., Shi, L., Li, D., Sun, Y., Niu, Y., Chen, Z., Luo, H., Pang, X., Sun, Z., Liu, C., Lv, A., Deng, Y., Larson-Rabin, Z., Wilkinson, M., Chen, S., 2012. Extensive pyrosequencing reveals frequent intra-genomic variations of Internal Transcribed Spacer Regions of Nuclear Ribosomal DNA. PLoS ONE 7, e43971.
Stadler, T., 2011. Mammalian phylogeny reveals recent diversification rate shifts. Proc. Natl. Acad. Sci. USA 108, 6187–6192.
Stamatakis, A., Hoover, P., Rougemont, J., 2008. A rapid bootstrap algorithm for the RAxML web-servers. Syst. Biol. 75, 758–771.
Stebbins, G.L., 1984. Polyploidy and the distribution of the arctic-alpine flora: new evidence and a new approach. Bot. Helv. 94, 1–13.
Suc, J.P., 1984. Origin and evolution of the Mediterranean vegetation and climate in Europe. Nature 307, 429–432.
Suchard, M.A., Weiss, R.E., Sinsheimer, J.S., 2001. Bayesian selection of continuous-time Markov Chain evolutionary models. Mol. Biol. Evol. 18, 1001–1013.
Szafer, W., 1961. Miocene flora from Stare Gliwice in upper Silesia. Pr. Inst. Geol. 33, 1–205.
Vaidya, G., Lohman, D.J., Meier, R., 2010. SequenceMatrix: concatenation software for the fast assembly of multi-gene datasets with character set and codon information. Cladistics 27, 171–180.
Valcárcel, V., 2008. Taxonomy, systematics and evolution of *Hedera* L. (Araliaceae). Dissertation, Universidad Pablo de Olavide.
Valcárcel, V., Vargas, P., 2010. Quantitative morphology and species delimitation under the general lineage concept: optimization for *Hedera* (Araliaceae). Am. J. Bot. 97, 1555–1573.
Valcárcel, V., Vargas, P., 2013. Phylogenetic reconstruction of key traits in the evolution of ivies (*Hedera* L.). Plant Syst. Evol. 229, 447–458.
Valcárcel, V., Fiz, O., Vargas, P., 2003. Chloroplast and nuclear evidence for multiple origins of polyploids and diploids of *Hedera* (Araliaceae) in the Mediterranean basin. Mol. Phylogen. Evol. 27, 1–20.
Vargas, P., McAllister, H.A., Morton, C., Jury, S.L., Wilkinson, M.J., 1999. Polyploid speciation in *Hedera* (Araliaceae): phylogenetic and biogeographic insights based on chromosome counts and ITS sequences. Plant Syst. Evol. 219, 165–179.
Verdú, M., Dávila, P., García-Fayos, P., Flores-Hernández, N., Valiente-Banuet, A., 2003. 'Convergent' traits of Mediterranean woody plants belong to pre-Mediterranean lineages. Biol. J. Linn. Soc. Lond. 78, 415–427.
Viguier, R., 1906. Recherches anatomiques sur la classification des Araliacées. Ann. Sci. Nat. Bot. IX (4), 1–210.
Wen, J., Plunkett, G.M., Mitchell, A.D., Wagstaff, S.J., 2001. The evolution of Araliaceae: a phylogenetic analysis based on ITS sequences of nuclear ribosomal DNA. Syst. Bot. 26, 144–167.
Wen, J., Lee, C., Lowry II, P.P., Hiep, N.T., 2003. Inclusion of the Vietnamese endemic genus *Grushvitzkya* in *Brassaiopsis* (Araliaceae): evidence from nuclear ribosomal ITS and chloroplast *ndh*F sequences. Bot. J. Linn. Soc. Lond. 142, 455–463.
Wen, J., Loc, P.K., Hiep, N.T., Regalado Jr., J., Averyanov, L.V., Lee, C., 2007. An unusual new species of *Trevesia* from Vietnam and its implications on generic delimitation in Araliaceae. Taxon 56, 1261–1268.
Wilgenbusch, J.C., Warren, D.L., Swofford, D.L., 2004. AWTY: a system for graphical exploration of MCMC convergence in Bayesian phylogenetic inference. <http://ceb.csit.fsu.edu/awty> (Last accessed 06.13).
Xie, W., Lewis, P.O., Fan, Y., Kuo, L., Chen, M.H., 2011. Improving marginal likelihood estimation for bayesian phylogenteic model selection. Syst. Biol. 60, 150–160.
Yang, Z., 2007. PAML 4: a program package for phylogenetic analysis by maximum likelihood. Mol. Biol. Evol. 24, 1586–1591.
Yang, Z., Rannala, B., 2006. Bayesian estimation of species divergence times under a molecular clock using multiple fossil calibrations with soft bounds. Mol. Biol. Evol. 23, 212–226.
Yi, T., Lowry II, P.P., Plunkett, G.M., Wen, J., 2004. Chromosomal evolution in Araliaceae and close relatives. Taxon 53, 987–1005.